Momentum-space calculation of vacuum polarisation effects for extended charge distributions

1988 J. Phys. A: Math. Gen. 21 3629

(http://iopscience.iop.org/0305-4470/21/18/016)

J. Phys. A: Math. Gen. 21 (1988) 3629-3642. Printed in the UK

Momentum-space calculation of vacuum polarisation effects for extended charge distributions

V Hnizdo

Department of Physics, Florida State University, Tallahassee, Florida 32306, USA and Department of Physics and Schonland Research Centre for Nuclear Sciences, University of the Witwatersrand, Johannesburg, South Africa†

Received 27 November 1987

Abstract. Vacuum polarisation potentials of extended charge distributions are calculated using an efficient Fourier-Bessel method for the evaluation of folding integrals. In order to obtain a well defined and a quantitatively correct picture of vacuum polarisation effects, these potentials are employed to yield vacuum polarisation charge densities via Poisson's equation of classical electrostatics.

1. Introduction

Quantum electrodynamics modifies the Coulomb interaction between two static charges by radiative corrections, which are usually interpreted as arising from the polarisation of virtual electron-positron pairs. These so-called vacuum polarisation effects are significant only at short distances, that is at distances shorter than the Compton wavelength of the electron. The usual explanation of the vacuum polarisation effects invokes a screening of an electric charge by the virtual electron-positron pairs, the screening being such that it becomes progressively less effective, and so the effective strength of the interaction increases, as the distance to charge decreases.

It is sometimes contended, however, that this intuitive picture of the vacuum as a polarisable medium is not correct, because the polarisation charge induced in the vacuum around, say, a positive electric charge looks in fact more like that induced by a negative charge in an ordinary dielectric, in that a positive charge induces around itself a positive vacuum polarisation charge. As an explanation of this strange behaviour, it could be then argued that vacuum polarisation should be pictured as arising from the interaction with negative-energy electrons and positrons in the Dirac sea. Negative-energy electrons should be seen as being repelled, and negative-energy positrons as attracted, by the positive charge that polarises the vacuum.

Thus conflicting pictures, such as those given in figure 1, can be found in the literature (e.g., see [1, 2]). These pictures obviously cannot refer to the same physical situation. Presumably, the distinction between the 'bare' and observed electric charges is important in this connection. It should be possible, however, to go beyond such qualitative and often ambiguous pictures by *calculating* polarisation charge densities from the vacuum polarisation potentials of observed, renormalised electric charges.

† Permanent address.

0305-4470/88/183629+14$02.50

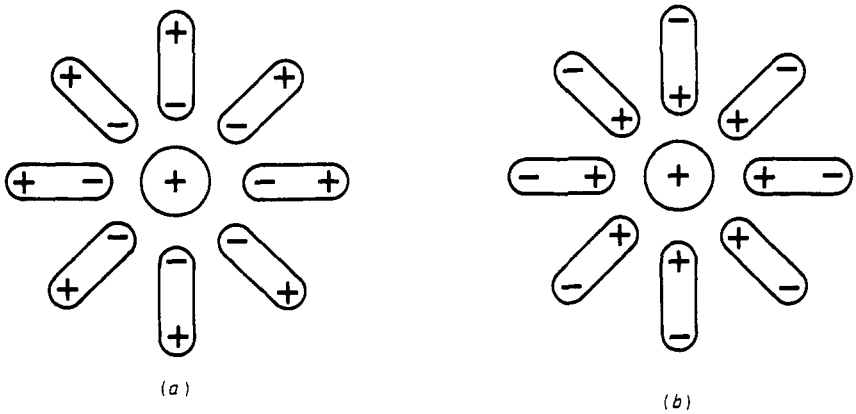

Figure 1. (*a*) A positive electric charge in the vacuum which is pictured as a polarisable medium of virtual electron–positron pairs (as, for example, in [1]). (*b*) A positive electric charge in the vacuum which is pictured as a polarisable sea of negative-energy electrons and positrons (as in [2]).

Polarisation charge densities obtained in such an unambiguous procedure should provide a quantitatively correct picture of vacuum polarisation effects.

The purpose of this paper is twofold. First, it is to employ the powerful momentum-space techniques that are available for an efficient and accurate evaluation of folding integrals in a calculation of vacuum polarisation potentials of extended charges, such as nuclear charge distributions, for which vacuum polarisation can be quite important in atomic and heavy-ion physics. Second, it is to provide a quantitatively correct picture of vacuum polarisation effects by calculating polarisation charge densities from these potentials using Poisson's equation of classical electrostatics. The case of a point-charge distribution can be then investigated as a limiting case of an extended charge distribution.

Sections 2–4 of this paper give the formalism for the calculation of the first-order vacuum polarisation energy, and its corresponding polarisation charge density, due to two extended charge distributions. In § 5, the numerical results for some typical nuclear charge distributions are presented. The results are discussed and conclusions are drawn in § 6.

2. Vacuum polarisation energy

The radiative correction to the Coulomb potential energy of two point electron charges e, separated by a distance r, is given to first order in the fine structure constant $\alpha = e^2/\hbar c = 1/137.036$ by the so-called Uehling potential [3]

$$U(r) = \frac{2\alpha e^2}{3\pi r}\chi_1(2r/\lambda\!\!\!^{-}_e). \tag{1}$$

Here, $\lambda\!\!\!^{-}_e = \hbar/m_e c = 386.159$ fm is the reduced Compton wavelength of the electron and the function $\chi_1(x)$ belongs to a class of functions defined by the integrals

$$\chi_n(x) = \int_1^\infty \mathrm{d}t\, \mathrm{e}^{-xt} t^{-n}(1+1/2t^2)(1-1/t^2)^{1/2}. \tag{2}$$

These functions can be expressed as [4]

$$\chi_n(x) = \mathrm{Ki}_{n-1}(x) - \tfrac{1}{2}\mathrm{Ki}_{n+1}(x) - \tfrac{1}{2}\mathrm{Ki}_{n+3}(x). \tag{3}$$

Here, the functions $\mathrm{Ki}_n(x)$ are defined [5] as repeated integrals of the modified Bessel function $K_0(x)$, and it follows from their properties that one can express the functions $\chi_n(x)$ in terms of the modified Bessel functions $K_0(x)$ and $K_1(x)$ and the Bessel integral $\mathrm{Ki}_1(x)$, for which accurate and efficient approximations in terms of Chebyshev polynomials are available [6]. Thus, for example, $\chi_1(x)$ is given as [4]

$$\chi_1(x) = \tfrac{1}{12}[(12+x^2)K_0(x) - x(10+x^2)K_1(x) + x(9+x^2)\mathrm{Ki}_1(x)]. \tag{4}$$

Similar expressions for other functions $\chi_n(x)$, $-3 \leq n \leq 4$, are given in [4].

The potential energy $V_2(\boldsymbol{r})$ of vacuum polarisation due to two charge distributions $Z_1\rho_1(\boldsymbol{r}_1)$ and $Z_2\rho_2(\boldsymbol{r}_2)$ is obtained by folding the Uehling potential with the two distributions such that

$$V_2(\boldsymbol{r}) = Z_1 Z_2 \int \mathrm{d}\boldsymbol{r}_1\, \mathrm{d}\boldsymbol{r}_2\, \rho_1(\boldsymbol{r}_1)\rho_2(\boldsymbol{r}_2)\, U(|\boldsymbol{r}+\boldsymbol{r}_1-\boldsymbol{r}_2|). \tag{5}$$

The coordinates are defined in figure 2. The densities $\rho_1(\boldsymbol{r}_1)$ and $\rho_2(\boldsymbol{r}_2)$ are assumed normalised to unity volume, and $Z_1 e$ and $Z_2 e$ are the total charges in the distributions. The potential energy due to an extended charge distribution and a point charge is then obtained when one of the distributions has a density given by the δ function

$$\rho(\boldsymbol{r}) = \delta^{(3)}(\boldsymbol{r}). \tag{6}$$

A δ function reduces the double-folding integral in equation (5) to a single-folding one. While essentially only single-folded potentials are going to be needed for the calculation of the vacuum polarisation charge density due to an extended charge distribution, the general formalism to be given here will cover the case of the vacuum polarisation energy due to two extended charge distributions.

A direct evaluation of the double-folding integral in equation (5) can be quite a difficult task, because it involves in general a six-dimensional integration. Only in the special case of a single folding over a spherically symmetric distribution can the

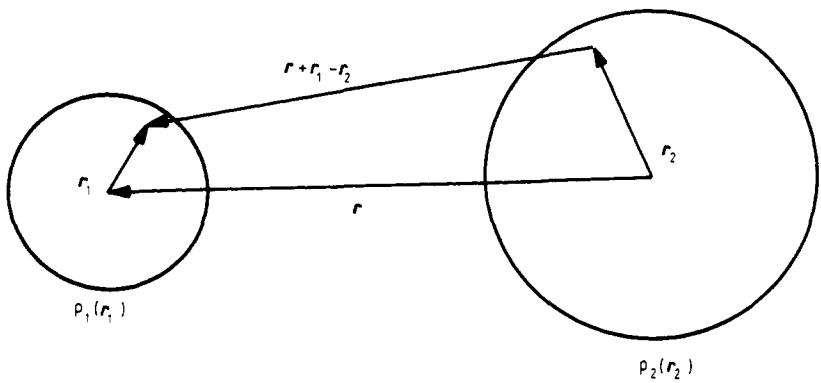

Figure 2. The coordinates used in equation (5) for the double folding over two distributions $\rho_1(\boldsymbol{r}_1)$ and $\rho_2(\boldsymbol{r}_2)$.

integration be reduced to a one-dimensional integral which, for a uniform charge distribution, can be solved in closed form [7]:

$$V_1(r)=\begin{cases}\dfrac{c}{r}\left(\dfrac{2r}{5\lambda\!\!\!^{-}_{\mathrm{e}}}+\dfrac{R}{2\lambda\!\!\!^{-}_{\mathrm{e}}}[\chi_3(x_1)-\chi_3(x_2)]+\frac{1}{4}[\chi_4(x_1)-\chi_4(x_2)]\right) & r\leqslant R\\ \dfrac{c}{r}\left(\dfrac{R}{2\lambda\!\!\!^{-}_{\mathrm{e}}}[\chi_3(x_1)+\chi_3(-x_2)]+\frac{1}{4}[\chi_4(x_1)-\chi_4(-x_2)]\right) & r>R.\end{cases} \tag{7}$$

Here, R is the radius of the uniform distribution, and the constant c and variables x_1 and x_2 are defined as

$$c=\frac{\alpha Ze^2}{2\pi}\left(\frac{\lambda\!\!\!^{-}_{\mathrm{e}}}{R}\right)^3 \qquad x_1=\frac{2(R+r)}{\lambda\!\!\!^{-}_{\mathrm{e}}} \qquad x_2=\frac{2(R-r)}{\lambda\!\!\!^{-}_{\mathrm{e}}} \tag{8}$$

where Ze is the total charge in the distribution. Equation (7) can be useful as an analytical check of the results that can be obtained for this special case by a general momentum-space procedure to be described in § 3.

3. Fourier integrals and Fourier–Bessel expansions

A function that is obtained by folding has a very useful property: its Fourier transform is simply the product of the Fourier transforms of the functions appearing in the folding integral (e.g., see [8]). This property is the basis of the momentum-space techniques for the evaluation of folding integrals. In the present problem, assuming spherically symmetric charge distributions, one needs only to know the Fourier transforms of the Uehling potential and the two distributions, to be able to reduce the double-folding integral of equation (5) to a one-dimensional Fourier integral:

$$V_2(r)=\frac{Z_1Z_2}{2\pi^2}\int_0^\infty \mathrm{d}k\,k^2\tilde{\rho}_1(k)\tilde{\rho}_2(k)\tilde{U}(k)j_0(kr). \tag{9}$$

The integrand involves the product of three Fourier transforms, each defined as

$$\tilde{f}(k)=\int \mathrm{d}\boldsymbol{r}f(r)\,\mathrm{e}^{\mathrm{i}\boldsymbol{k}\cdot\boldsymbol{r}}=4\pi\int_0^\infty \mathrm{d}r\,r^2f(r)j_0(kr). \tag{10}$$

Equation (9) is just the Fourier transform of the double-folding integral from the momentum space (k-space) back to the r-space. The Fourier transforms are expressed in terms of the spherical Bessel function $j_0(x)$ because the functions involved are assumed to be spherically symmetric. One can generalise equation (9) easily for non-spherical distributions [9].

The use of Fourier transforms in the present problem is particularly attractive, because the Fourier transform of the Uehling potential of equation (1) can be expressed in terms of elementary functions

$$\tilde{U}(k)=\frac{4\alpha e^2}{3k^2}\left[\left(1-\frac{2}{\lambda\!\!\!^{-2}_{\mathrm{e}}k^2}\right)\left(s\ln\frac{s+1}{s-1}-2\right)+\frac{1}{3}\right] \tag{11a}$$

where

$$s=[1+(2/\lambda\!\!\!^{-}_{\mathrm{e}}k)^2]^{1/2}. \tag{11b}$$

This result is obtained by performing the integration involved in the definition of the function $\chi_1(x)$ (see equation (2)) only after first Fourier-transforming the function $\exp(-2rt/\lambda\!\!\!^{-}_e)/r$. The Fourier transforms of the functional forms that are most often used for nuclear charge distributions are also known analytically (see § 5). In any case, it is not difficult to calculate the Fourier transform of a charge distribution numerically, because the radial integral in equation (10) converges rapidly for a distribution of a limited radial extension.

Some use of Fourier transforms for the calculation of the vacuum polarisation potential of two extended charge distributions has been described in [10].

In practice, the folded potential is required for only a limited range of the radial coordinate r. The Fourier integral of equation (9) can be then replaced by a series expansion by employing a Fourier-Bessel expansion [11] of the Uehling potential:

$$U(r) = \sum_{n=1}^{\infty} c_n j_0(k_n r). \tag{12}$$

Such an expansion is valid only within some maximum radius R and the discrete values k_n are such that $k_n R$ are the positive roots of

$$aj_0(x) + bx\, \mathrm{d}j_0(x)/\mathrm{d}x = 0. \tag{13}$$

The expansion of equation (12) is the simplest when the roots of equation (13) are taken either as $n\pi$ (that is when $b = 0$ in equation (13)) or as $(2n-1)\pi/2$ (when $a = b$). Then the coefficients c_n in equation (12) are given by

$$c_n = \frac{2k_n^2}{R}\int_0^R \mathrm{d}r\, r^2 U(r) j_0(k_n r) = \frac{4\alpha e^2 k_n}{3\pi R}\int_0^R \mathrm{d}r\, \chi_1(2r/\lambda\!\!\!^{-}_e)\sin k_n r \tag{14a}$$

where

$$k_n = n\pi/R \qquad \text{or} \qquad k_n = \tfrac{1}{2}(2n-1)\pi/R. \tag{14b}$$

On writing the Fourier-Bessel expansion of the Uehling potential as

$$U(|\boldsymbol{r} + \boldsymbol{r}_1 - \boldsymbol{r}_2|) = \frac{1}{4\pi}\sum_{n=1}^{\infty} c_n \int \mathrm{d}\hat{\boldsymbol{k}}_n\, \mathrm{e}^{\mathrm{i}\boldsymbol{k}_n\cdot(\boldsymbol{r}+\boldsymbol{r}_1-\boldsymbol{r}_2)} \tag{15}$$

where use is made of the identity

$$4\pi j_0(ks) = \int \mathrm{d}\hat{\boldsymbol{k}}\, \mathrm{e}^{\mathrm{i}\boldsymbol{k}\cdot\boldsymbol{s}} \tag{16}$$

the double-folding integral in equation (5) is reduced immediately to a Fourier-Bessel series:

$$V_2(r) = Z_1 Z_2 \sum_{n=1}^{\infty} c_n \tilde{\rho}_1(k_n)\tilde{\rho}_2(k_n) j_0(k_n r). \tag{17}$$

The great advantage of equation (17) is that it replaces the Fourier integral of equation (9), which, in general, has to be evaluated numerically, by a discrete sum in which essentially only the number of terms controls the degree of approximation to the exact value of the folding integral. For the expansion of equation (17) to be valid for r up to some $r_{\max}$, the radius R of the expansion of the Uehling potential must be at least

$$R = r_{\max} + R_1 + R_2 \tag{18}$$

where R_1 and R_2 are the radii beyond which the charge distributions $\rho_1(r)$ and $\rho_2(r)$ can be considered as negligible, respectively. It should be stressed that the coefficients c_n in equation (17), defined by equation (14), involve the Fourier transform of the Uehling potential taken only up to $r = R$. This is somewhat unfortunate in the present case, because it does not seem to be possible to evaluate the finite-radius Fourier transform of the Uehling potential in closed form. However, this circumstance is still greatly outweighed by the advantages of the discrete-momentum formulation. Using the finite-radius Fourier transform

$$\int_0^R \mathrm{d}r\, r^2 \frac{\mathrm{e}^{-\mu r}}{r} j_0(kr) = \frac{1}{k^2+\mu^2}\{1-\mathrm{e}^{-\mu R}[\cos kR + (\mu/k)\sin kR]\} \tag{19}$$

with $\mu = 2t/\lambda\!\!\!^{-}_{\mathrm{e}}$, one obtains for the expansion coefficients of equation (14):

$$c_n = \frac{2k_n^2}{R}\left[\frac{1}{4\pi}\tilde{U}(k_n) + (-1)^n \frac{\alpha e^2 \lambda\!\!\!^{-}_{\mathrm{e}}}{3\pi k_n} I\left(\frac{2R}{\lambda\!\!\!^{-}_{\mathrm{e}}}, \frac{\lambda\!\!\!^{-}_{\mathrm{e}} k_n}{2}\right)\right] \tag{20a}$$

with

$$k_n = \tfrac{1}{2}(2n-1)\pi/R. \tag{20b}$$

Here, the finite-radius correction to the Fourier transform of the Uehling potential $\tilde{U}(k_n)$, given by equation (11), is expressed in terms of the integral

$$\begin{aligned} I(\mu, \nu) &= \int_1^\infty \mathrm{d}t \frac{\mathrm{e}^{-\mu t}}{\nu^2+t^2}(1+1/2t^2)(1-1/t^2)^{1/2} \\ &= \int_0^{\pi/2} \mathrm{d}\theta \frac{\mathrm{e}^{-\mu/\cos\theta}}{\nu^2\cos^2\theta+1}(1+\tfrac{1}{2}\cos^2\theta)\sin^2\theta. \end{aligned} \tag{21}$$

For large values of ν, this integral has an asymptotic expansion

$$I(\mu, \nu) \sim \frac{1}{\nu^2}\sum_{n=0}^{\infty} \chi_{-2n}(\mu)\frac{(-1)^n}{\nu^{2n}}. \tag{22}$$

Reference [10] gives a recursive scheme for the calculation of the functions $\chi_n(x)$ with $n \leqslant -3$. However, for all the values of ν and μ of our interest, the integral $I(\mu, \nu)$ is easily evaluated with a good accuracy by a direct numerical quadrature. In any case, the finite-radius corrections are relatively small when the radius R is not too small, and in a given expansion one needs to evaluate only $n_{\max}$ of such integrals, where $n_{\max}$ is the number of the expansion terms required.

At very small distances, the Uehling potential is approximated asymptotically as [3]

$$U(r) \approx \frac{2\alpha \mathrm{e}^2}{3\pi r}\left(\ln\frac{\lambda\!\!\!^{-}_{\mathrm{e}}}{r} - \gamma - \tfrac{5}{6}\right) \tag{23}$$

where $\gamma = 0.5772\ldots$ is Euler's constant, and in this approximation one can evaluate the coefficients of equation (14) in closed form:

$$c_n \approx \frac{4\alpha e^2}{3\pi R}\left[\left(\ln\frac{\lambda\!\!\!^{-}_{\mathrm{e}}}{R} - \gamma - \tfrac{5}{6}\right)(1-\cos k_n R) + \ln(k_n R) - \mathrm{Ci}(k_n R) + \gamma\right]. \tag{24}$$

Here, $\mathrm{Ci}(x)$ is the cosine integral (for approximations of $\mathrm{Ci}(x)$ see [6, p 116]):

$$\mathrm{Ci}(x) = \gamma + \ln x + \int_0^x \mathrm{d}t(\cos t - 1)/t. \tag{25}$$

Unfortunately, for good accuracy, the approximation of equation (24) requires an expansion radius R that is not too small only on the nuclear scale.

The use of a discrete-momentum representation for the calculation of folded nuclear potentials has been described in [12].

4. Polarisation charge density

The vacuum polarisation charge density that corresponds to a given vacuum polarisation potential can be calculated as the charge density which would produce the potential according to the laws of classical electrostatics. The charge density $\rho(r)$ that gives rise to a spherically symmetric potential energy $V(r)$ is given by the radial Poisson's equation:

$$\rho(r) = -\frac{1}{4\pi e}\nabla^2 V(r) = -\frac{1}{4\pi e}\left(\frac{2\,\mathrm{d}V(r)}{r\,\mathrm{d}r} + \frac{\mathrm{d}^2 V(r)}{\mathrm{d}r^2}\right). \tag{26}$$

When the potential energy $V(r)$ is obtained by a double folding over two extended charge distributions, one should not confuse the potential-energy equivalent density $\rho(r)$ of equation (26), which is spherically symmetric, with the non-spherical distribution corresponding to a given two-centre configuration of the two extended charges.

Thus to calculate the polarisation charge density, one requires the first and second derivatives of the vacuum polarisation potential. These are obtained easily by differentiating with respect to r the Fourier integral or the Fourier–Bessel series for the potential, equations (9) or (17), under the integral sign or term by term, respectively. The required derivatives of the spherical Bessel function $j_0(x)$ are:

$$\mathrm{d}j_0(x)/\mathrm{d}x = -j_1(x) \qquad \mathrm{d}^2 j_0(x)/\mathrm{d}x^2 = j_2(x) - j_1(x)/x. \tag{27}$$

According to Gauss's law of electrostatics, the polarisation charge within a sphere of radius r is given in terms of the first derivative of the spherically symmetric potential as follows:

$$q(r) = 4\pi \int_0^r \mathrm{d}r'\, r'^2 \rho(r') = -\frac{r^2}{e}\frac{\mathrm{d}V(r)}{\mathrm{d}r}. \tag{28}$$

The total amount of the polarisation charge, $q(r)$ as $r \to \infty$, is zero.

5. Application and results

The nuclear charge distributions of light nuclei are usually modelled by the modified harmonic-oscillator density:

$$\rho_{\mathrm{H}}(r) = \rho_0(1 + b^2 r^2)\,\mathrm{e}^{-c^2 r^2} \tag{29a}$$

where

$$\rho_0 = \frac{2c^5}{\pi^{3/2}(2c^2 + 3b^2)} \tag{29b}$$

while those of medium-mass and heavy nuclei are most often modelled by the Fermi density:

$$\rho_{\mathrm{F}}(r) = \rho_0(1 + \mathrm{e}^{(r-R)/a})^{-1} \tag{30a}$$

where

$$\rho_0 = \frac{3}{4\pi R^3}\left[1 + \left(\frac{\pi a}{R}\right)^2 - 6\left(\frac{a}{R}\right)^3 \sum_{n=1}^{\infty} (-1)^n \frac{\mathrm{e}^{-nR/a}}{n^3}\right]^{-1}. \tag{30b}$$

The constants ρ_0 normalise the densities to unity volume. The Fourier transform of the density of equation (29) is

$$\tilde{\rho}_H(k) = \left(1 - \frac{b^2k^2}{2c^2(2c^2+3b^2)}\right) e^{-k^2/4c^2} \tag{31}$$

and that of the Fermi density of equation (30) [9]:

$$\tilde{\rho}_F(k) = \frac{8\pi\rho_0}{k^3}(2t^2 \cosh x \sin kR - tkR \cos kR) - 8\pi a^3\rho_0 \sum_{n=1}^{\infty} (-1)^n \frac{n\, e^{-nR/a}}{(n^2+a^2k^2)^2} \tag{32a}$$

where

$$t = x/2 \sinh x \qquad x = \pi ka. \tag{32b}$$

The Fourier transform of the δ function, equation (6), is simply a constant equal to unity, while that of the uniform density of radius R, normalised to unity volume, is

$$\tilde{\rho}_R(k) = \frac{3}{kR} j_1(kR). \tag{33}$$

The uniform density can be regarded as the limit $a \to 0$ of the Fermi distribution of equation (30).

As examples, the potential energies of vacuum polarisation and the corresponding polarisation charge densities were calculated for the nuclei ^{16}O and ^{208}Pb. The Fourier-Bessel expansion given by equations (17), (20) and (21) was used for the calculation of the potential energy, and the polarisation charge density was then obtained according to equation (26). A modified harmonic oscillator density with parameters $b = 0.678$ fm^{-1} and $c = 0.546$ fm^{-1} (root mean square radius $\langle r^2\rangle^{1/2} = 2.72$ fm) was used for the charge distribution of ^{16}O, and a Fermi density with parameters $R = 6.62$ fm and $a = 0.549$ fm ($\langle r^2\rangle^{1/2} = 5.52$ fm) for ^{208}Pb [13]. For a six-digit accuracy in the potential energy and a three-digit accuracy in the polarisation charge density, about 40 terms in the Fourier-Bessel expansion were required in the radial range $r < 20$ fm considered.

Figure 3 gives the calculated vacuum polarisation energy and vacuum polarisation charge density for the system $e^+ + {}^{16}O$, which requires only a single folding. The energy is shown there both absolutely and as a ratio to the Uehling potential of equivalent point charges. The results for the realistic nuclear charge distribution are there compared also with those for a uniform nuclear charge density of radius $R = 3.51$ fm, which has the same mean square radius as the realistic charge distribution. The calculation with the uniform nuclear density was done using the closed expression of equation (7) and the derivatives $d\chi_n(x)/dx = -\chi_{n-1}(x)$. Figure 4 presents in the same fashion the double-folding results for the system $^{16}O + {}^{16}O$. Here, all the calculations were performed using the Fourier-Bessel expansion.

The results of similar calculations for the systems $e^+ + {}^{208}Pb$ and $^{16}O + {}^{208}Pb$ are shown in figures 5 and 6, respectively. The radius of the uniform charge density of ^{208}Pb was taken as $R = 7.13$ fm to reproduce the mean square radius of its realistic charge distribution. It should be pointed out, however, that higher than first-order vacuum polarisation effects [7], which are neglected here, could become significant for a charge as large as that of the Pb nucleus.

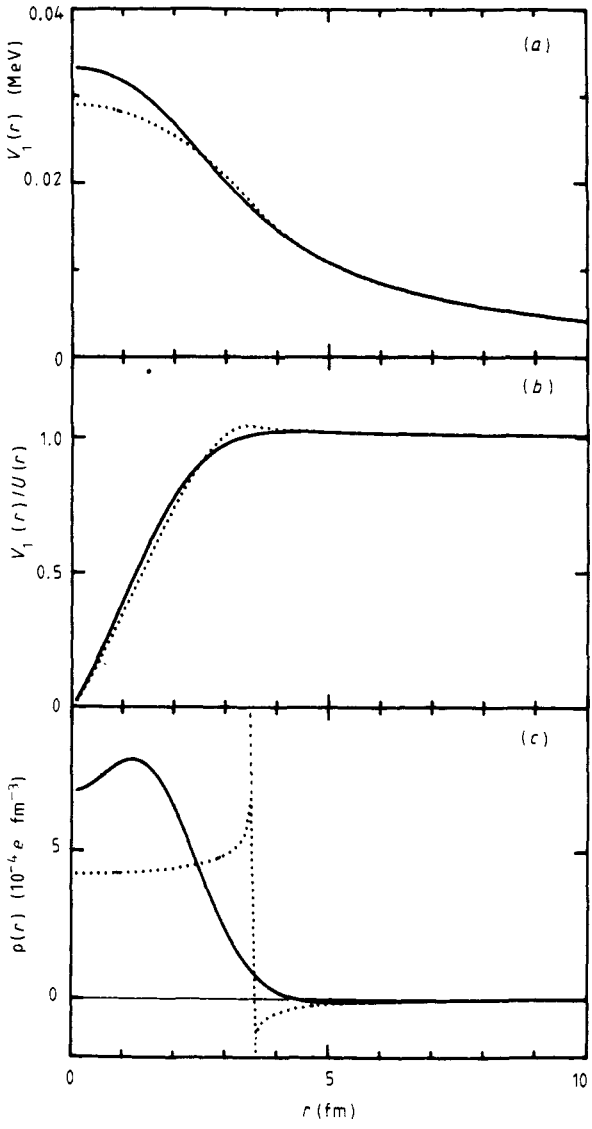

Figure 3. The system $e^+ + {}^{16}O$. (*a*) The vacuum polarisation energy $V_1(r)$ as a function of the separation between the centres of the two charges. (*b*) The ratio of $V_1(r)$ to the vacuum polarisation energy of equivalent point charges, $U(r)$. (*c*) The polarisation charge density $\rho(r)$ corresponding to the energy $V_1(r)$. The full curves are for the calculations with a realistic charge distribution of the nucleus ^{16}O and the dotted curves for those with a uniform charge density of the same mean square radius as the realistic distribution (see the text).

6. Discussion and conclusions

One can see from these results that the folding over the nuclear charge distributions modifies significantly the point vacuum polarisation energy only at distances close to or smaller than the sum of the root mean square radii of the two charge distributions. While these finite-size effects are relatively important in muonic atoms [14], they cannot

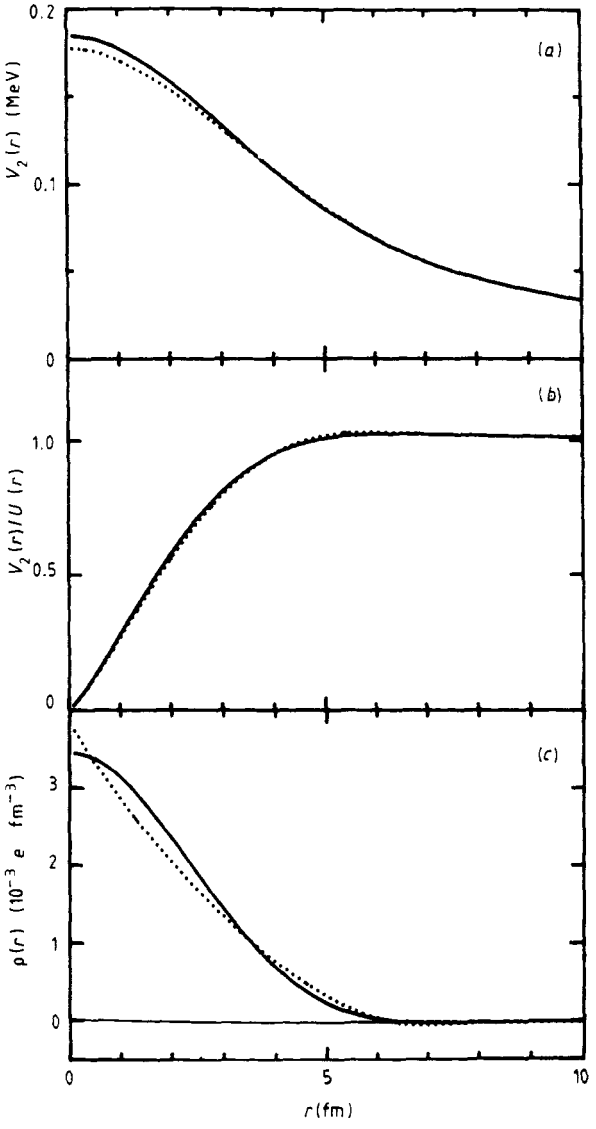

Figure 4. The system $^{16}O+^{16}O$. (*a*) The vacuum polarisation energy $V_2(r)$ as a function of the separation between the centres of the two charges. (*b*) The ratio of $V_2(r)$ to the vacuum polarisation energy of equivalent point charges, $U(r)$. (*c*) The polarisation charge density $\rho(r)$ corresponding to the energy $V_2(r)$. The full curves are for the calculations with a realistic charge distribution of the nucleus ^{16}O and the dotted curves for those with a uniform charge density of the same mean square radius as the realistic distribution (see the text).

play any significant role in heavy-ion scattering because of the predominance of the nuclear interaction and strong absorption in heavy-ion systems at these distances.

The results obtained for the polarisation charge densities are instructive. The single-folding calculations presented in figures 3(*c*) and 5(*c*) give directly the vacuum polarisation charge densities due to the nuclear charge distributions of ^{16}O and ^{208}Pb, respectively. The essential feature of these polarisation charge densities is that a

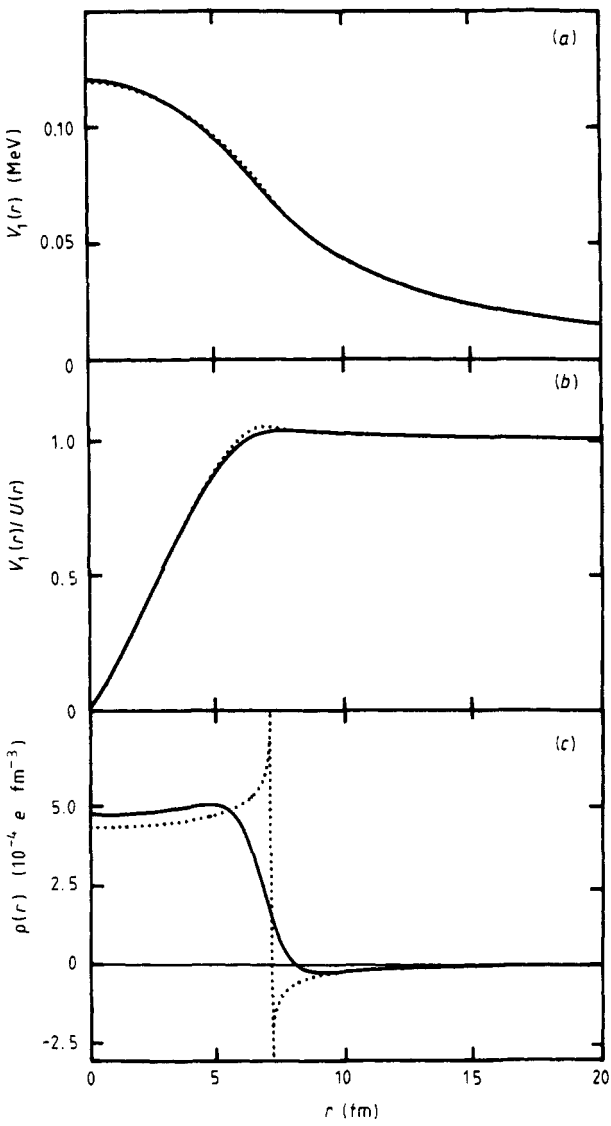

Figure 5. The system $e^+ + {}^{208}Pb$. (*a*) The vacuum polarisation energy $V_1(r)$ as a function of the separation between the centres of the two charges. (*b*) The ratio of $V_1(r)$ to the vacuum polarisation energy of equivalent point charges, $U(r)$. (*c*) The polarisation charge density $\rho(r)$ corresponding to the energy $V_1(r)$. The full curves are for the calculations with a realistic charge distribution of the nucleus ^{208}Pb and the dotted curves for those with a uniform charge density of the same mean square radius as the realistic distribution (see the text).

positive charge is induced within the inducing positive charge distribution, while a negative charge is induced outside it. Thus there is some resemblance to the counter-intuitive features of the sketch in figure 1(*b*). It should be stressed, however, that the polarisation charge densities obtained in the present procedure are those of observed, that is already renormalised, electric charges. The 'bare' charge that polarises the vacuum is the observed positive charge plus the positive polarisation charge that is

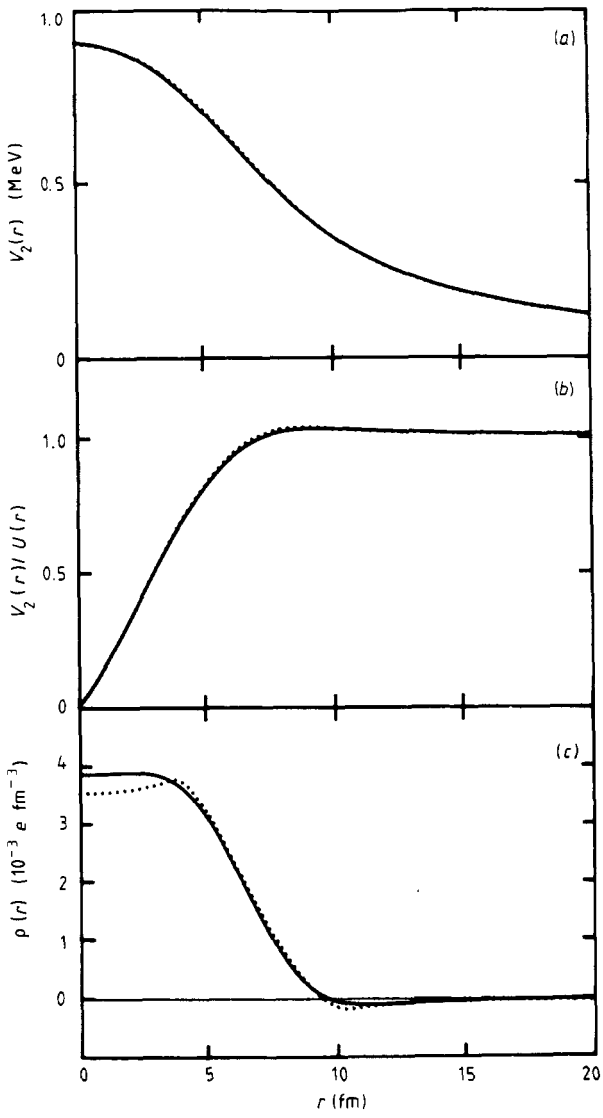

Figure 6. The system $^{16}O+^{208}Pb$. (*a*) The vacuum polarisation energy $V_2(r)$ as a function of the separation between the centres of the two charges. (*b*) The ratio of $V_2(r)$ to the vacuum polarisation energy of equivalent point charges, $U(r)$. (*c*) The polarisation charge density $\rho(r)$ corresponding to the energy $V_2(r)$. The full curves are for the calculations with realistic charge distributions of the nuclei ^{16}O and ^{208}Pb and the dotted curves for those with uniform charge densities of the same mean square radii as the realistic distributions (see the text).

calculated as induced within it. The counter-intuitive induction of a positive charge inside a positive inducing charge is simply a formal consequence of our use of *renormalised* electric charges in calculating the polarisation charge density.

The vacuum-polarisation charge density due to a point charge can be investigated now most easily as a limit of that of an extended charge, which can be taken for simplicity as having a uniform density distribution. The polarisation charge density

$\rho(r)$ of a uniform charge distribution of radius R has a singularity at $r = R$: as $r \to R\pm$, the density $\rho(r) \to \mp\infty$ (cf the polarisation charge densities of uniform charge distributions for ^{16}O and ^{208}Pb, given by the dotted lines in figures 3(*c*) and 5(*c*), respectively). As the radius R decreases, the singlarity in the polarisation charge density at $r = R$ moves closer to $r = 0$. In the limit $R \to 0$, the polarisation charge density becomes highly singular at $r = 0$: for $r \to 0+$ the density approaches $-\infty$ as $-r^{-3}$, while at exactly $r = 0$ there must remain after an integration a positive logarithmic divergence, which keeps the total induced charge at zero. Formally, for very small r, one can write the polarisation charge density due to a point charge e, i.e. the Uehling polarisation density, as follows:

$$\rho_U(r) \approx \lim_{\varepsilon \to 0} \frac{\alpha e}{6\pi^2}\left[\left(\ln\frac{\lambda\!\!\!^{-}_e}{r+\varepsilon} - \gamma - \tfrac{4}{3}\right)\frac{\delta(r)}{r^2} - \frac{1}{(r+\varepsilon)^3}\right]. \tag{34}$$

Here, $\delta(r)$ is the one-dimensional δ function and the limit $\varepsilon \to 0$ is understood to be taken after any integration. One can check easily that this density satisfies equation (28) for the cumulative polarisation charge when the asymptotic approximation for the point-charge Uehling potential, given by equation (23), is used.

The 'bare' point charge that corresponds to an observed point charge e is then infinitely large, as it is the sum of e and the charge that is calculated as induced at $r = 0$, which is logarithmically divergent, being given by the integral of the first term in equation (34). The polarisation charge induced by the point charge in the region $0 < r < \infty$ is logarithmically infinite too, but of the opposite sign. The total charge within a sphere of radius $r \gg \lambda\!\!\!^{-}_e$, which is the sum of the 'bare' charge and the charge induced outside $r = 0$, is the observed charge e. The subtraction of infinities in the renormalisation of a point electric charge in quantum electrodynamics can be thus explicitly exhibited.

To conclude, vacuum polarisation potentials of extended charge distributions have been calculated efficiently by using a discrete momentum-space method based on Fourier-Bessel expansions for the evaluation of folding integrals. A well defined and quantitatively correct picture of vacuum polarisation effects has been obtained by using the procedure of calculating polarisation charge densities via Poisson's equation of classical electrostatics.

Acknowledgments

The author wishes to thank W D Heiss for suggesting this problem. The support of this work by the National Science Foundation, USA, and the receipt of a sabbatical grant from the Foundation for Research Development, South Africa, are gratefully acknowledged.

References

[1] Aitchison I J R and Hey A J G 1982 *Gauge Theories in Particle Physics* (Bristol: Adam Hilger) p 281
[2] Greiner W, Müller B and Rafelski J 1985 *Quantum Electrodynamics of Strong Fields* (Berlin: Springer) p 4

[3] Berestetskii V B, Lifshitz E M and Pitaevskii L P 1982 *Quantum Electrodynamics* (Oxford: Pergamon) p 504
[4] Klarsfeld S 1977 *Phys. Lett.* **66B** 86
[5] Abramowitz M and Stegun I A 1964 *Handbook of Mathematical Functions* (Washington: National Bureau of Standards) p 483
[6] Luke Y L 1975 *Mathematical Functions and their Approximations* (New York: Academic) p 328
[7] Huang K N 1976 *Phys. Rev.* A **14** 1311
[8] Messiah A 1961 *Quantum Mechanics* vol 1 (Amsterdam: North-Holland) p 476
[9] Krappe H J 1976 *Ann. Phys., NY* **99** 142
[10] Roesel F, Trautmann D and Viollier R D 1977 *Nucl. Phys.* A **292** 523
[11] Gray A and Mathews G B 1966 *A Treatise on Bessel Functions and Their Applications to Physics* (New York: Dover) p 91
[12] Petrovich F 1975 *Nucl. Phys.* A **251** 143
[13] de Jager C W, de Vries H and de Vries C 1974 *At. Data Nucl. Data Tables* **14** 479
[14] Rinker G A and Wilets L 1975 *Phys. Rev.* A **12** 748